proceedings

MDPI

Proceedings

Anti- and Hyper-Nuclei Production at the LHC with ALICE †

Luca Barioglio, on behalf of the ALICE Collaboration

Department of Physics, Università degli Studi di Torino, via P. Giuria 1, 10125 Torino (TO), Italy; luca.barioglio@cern.ch

† Presented at Hot Quarks 2018—Workshop for Young Scientists on the Physics of Ultrarelativistic Nucleus-Nucleus Collisions, Texel, The Netherlands, 7–14 September 2018.

Published: 7 May 2019

Abstract: At the Large Hadron Collider (LHC) a significant production of (anti-)(hyper-)nuclei is observed in proton-proton (pp), proton-lead (p-Pb) and lead-lead (Pb-Pb) collisions. The measurement of the production yields of light (anti-)nuclei is extremely important to provide insight into the production mechanisms of nuclear matter, which is still an open question in high energy physics. The outstanding particle identification (PID) capabilities of the ALICE detectors allow the identification of rarely produced particles such as deuterons, ^{3}He and their antiparticles. From the production spectra measured for light (anti-)nuclei with ALICE, the key observables of the production mechanisms (antimatter/matter ratio, coalescence parameter, nuclei/protons ratio) are computed and compared with the available theoretical models. Another open question is the determination of the hypertriton lifetime: published experimental values show a lifetime shorter than the expected one, which should be close to that of the free Λ hyperon. Thanks to the high-resolution track reconstruction capabilities of the ALICE experiment, it has been possible to determine the hypertriton lifetime at the highest Pb-Pb collisions energy with the highest precision ever reached.

Keywords: nuclei; antinuclei; hypertriton lifetime

1. Introduction

At the LHC, (anti-)nuclei are abundantly produced in different collision systems and at different energies. Since light nuclei are characterised by a low binding energy ($E_B \sim 2$ MeV) compared to the temperature of the chemical freeze-out, which is the phase when the abundances of the particle species are fixed ($T_{ch} \sim 160$ MeV), the study of the nuclear (anti-)matter production mechanisms is crucial to understand how these loosely bound objects can be produced in such extreme conditions.

The study of the production mechanisms is carried out comparing the experimental results with the predictions of the available phenomenological models, namely the statistical-thermal [1] and the coalescence [2] models. According to the statistical thermal model, (anti-)nuclei are produced at the chemical freeze-out in statistical equilibrium, as well as all the other hadrons.

On the other hand, in the coalescent picture, nucleons that are close to each other in the phase space after the chemical freeze-out can merge and form a nucleus via coalescence.

At the LHC energies not only (anti-)nuclei, but also (anti-)hypernuclei are produced. In particular, the ALICE experiment measured the production of $^3_\Lambda$H (hypertriton) in Pb-Pb collisions. A hypernucleus is a nucleus that contains at least one hyperon in addition to the nucleons and the hypertriton is the lightest hypernucleus, consisting of a bound state of a neutron, a proton and a Λ hyperon. The measurement of the hypertriton lifetime is extremely important because it can give an insight of the internal structure of this hypernucleus and because the latest measurements showed a slight disagreement with the theoretical predictions [3–5], which are close to the free Λ lifetime.

This disagreement is known as the *hypertriton lifetime puzzle*. These analyses are based on data collected by ALICE and the description of the detectors can be found in [6].

2. (Anti-)Nuclei Production

The ALICE experiment has observed the production of nuclei in different collision systems and at different energies. In particular, the transverse momentum spectra have been measured for deuterons and ^{3}H in pp collisions at $\sqrt{s} = 7$ TeV, in p-Pb collisions at $\sqrt{s_{NN}} = 5$ TeV and in Pb-Pb collisions at $\sqrt{s_{NN}} = 2.76$ TeV [7]. For deuterons, the production spectra have also been measured in pp collisions at $\sqrt{s} = 13$ TeV. The spectra have been measured both for nuclei and antinuclei. The ratio between the spectra of antinuclei and nuclei is important to understand whether there is a difference in the production of matter and antimatter. The ratios have been evaluated both for deuterons and ^{3}He for all the measurements aforementioned and they are always compatible with the unity within the uncertainties. An example of the ratio between the spectra of antideuterons and deuterons is reported in in Figure 1. The results are obtained from pp collisions at $\sqrt{s} = 13$ TeV. The ratios are presented for different multiplicity classes, going from the highest (I) to the lowest (X) multiplicity.

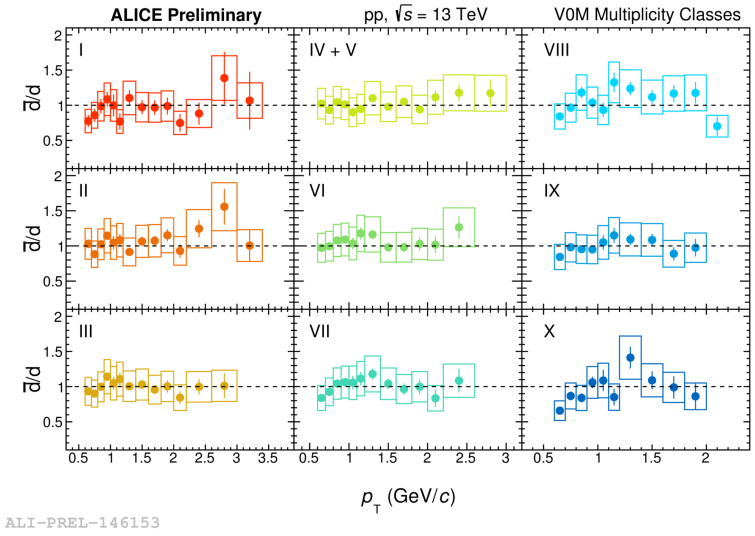

Figure 1. Ratio between the spectra of antideuterons and deuterons.

By comparing the p_{T} spectra of nuclei and protons, two important observables can be computed: the coalescence parameter B_A and the ratio between the yields of nuclei and protons. The coalescence parameter is a quantity related to the probability of forming a nucleus via coalescence and it is defined as:

$$B_A(p_{\mathrm{T}}^p) = \frac{\frac{1}{2\pi p_{\mathrm{T}}^A}\frac{\mathrm{d}^2 N_A}{\mathrm{d}p_{\mathrm{T}}^A \mathrm{d}y}}{\left(\frac{1}{2\pi p_{\mathrm{T}}^p}\frac{\mathrm{d}^2 N_p}{\mathrm{d}p_{\mathrm{T}}^p \mathrm{d}y}\right)^A}, \qquad with \quad p_{\mathrm{T}}^p = p_{\mathrm{T}}^A / A \tag{1}$$

where A is the mass number of the nucleus, p_{T}^p and p_{T}^A are the proton and the nucleus transverse momentum respectively. Here the case of deu9terons is discussed and the latest ALICE results of the B_2 and the d/p are shown.

The B_2 as a function of p_{T} is computed for all the collision systems and energies listed above. In order to compare the B_2 in the different collision systems, the value obtained for each of these at $p_{\mathrm{T}}/A = 0.75$ GeV/c is plotted as a function of the event multiplicity (Figure 2). This particular p_{T} bin ($[0.7; 0.8]$ GeV/c) has been chosen because it is common between all the analyses. However, the evolution of the B_2 with the multiplicity is very similar in the other p_{T} bins. The coalescence parameter evolves smoothly with the event multiplicity, without any discontinuity passing from a colliding system to another, suggesting a common production mechanism between small and large

systems that depends only on the event multiplicity and consequently on the size of the collision system. Two kinds of regimes can be distinguished. At low multiplicity, the coalescence parameter is slightly decreasing, while at high multiplicity it decreases more quickly. A possible explanation is that at low multiplicities the system size is comparable with the deuteron size, while increasing the multiplicity the system size becomes larger and larger and the probability to form a nucleus via coalescence becomes smaller.

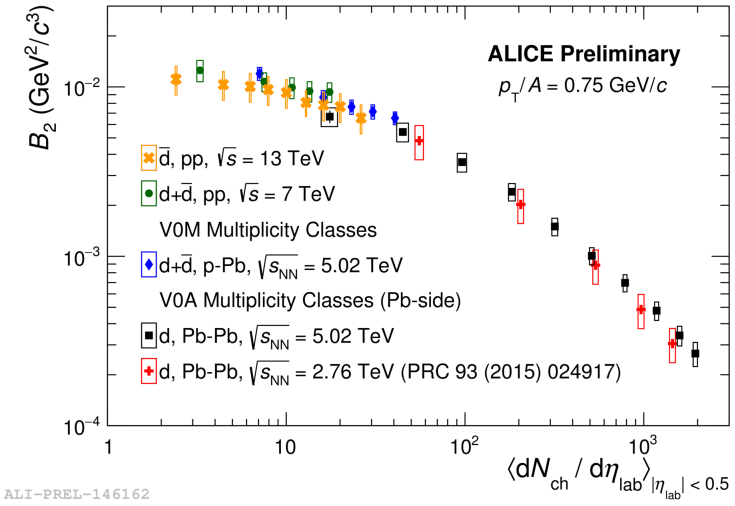

Figure 2. Coalescence parameter B_2 at $p_T/A = 0.75$ GeV/c as a function of multiplicity.

A similar behaviour is seen for the ratio between the p_T-integrated yields of deuterons and protons as a function of multiplicity (Figure 3). The deuteron and proton spectra are fitted with a Levy-Tsallis distribution [8] in pp collisions and with a Blast-Wave function [9] in p-Pb and Pb-Pb collisions, in order to extrapolate the yields in the unmeasured regions at low and high p_T and integrate over the full p_T range. The ratio evolves smoothly with the multiplicity and it shows no discontinuity between different collision systems and different energies. Generally, for small systems the ratio is increasing, in agreement with the predictions of the coalescence model, while for larger systems such as Pb-Pb the ratio is flat, in agreement with the predictions of the thermal model.

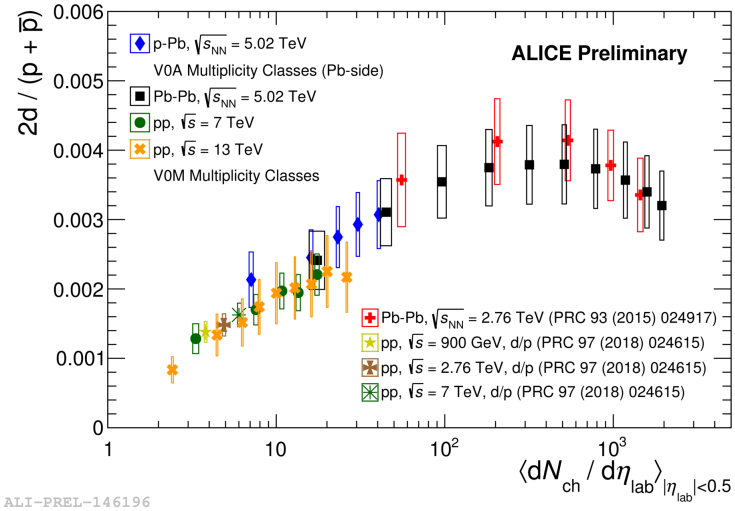

Figure 3. Ratio between the deuteron and proton yields as a function of the event multiplicity.

In conclusion, the thermal model provides a better description of the experimental data in large systems, while the coalescence model works well for small systems. However, the smooth evolution of the B_2 and the d/p suggests a system size dependent common production mechanism..

3. The Hypertriton Lifetime

The hypertriton is characterised by a low Λ separation energy ($E_B = 130$ keV) and for this reason the lifetime is expected to be close to that of the free Λ [3–5]. Over time, several measurements have been carried out. They can be grouped according to the experimental techniques: visualising and ion-beam based. The former, like bubble chambers and emulsions, give results compatible within 1 σ with the free Λ lifetime, but these measurements have large uncertainties. The latter, relaying on large data samples, have lower uncertainties and are slightly but systematically below the predicted value. The ALICE collaboration measured the hypertriton lifetime via the two-body mesonic decay channel ${}^3_\Lambda H \longrightarrow {}^3 He + \pi$ in the Pb-Pb data sample at $\sqrt{s_{NN}} = 5$ TeV. The result is the most precise ever obtained and it is compatible within 1 σ both with the world average and the free Λ lifetime. Recently the STAR collaboration published a lower value, but compatible within 2 σ with the ALICE result. More precise measurements will be possible with the large data samples that have been collected in the 2018 Pb-Pb acquisition and that will be collected during Run 3.

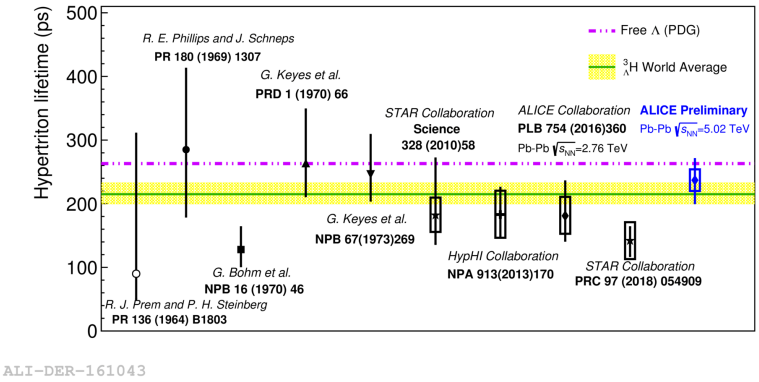

Figure 4. Collection plot of hypertriton lifetime measurements. In blue the latest ALICE results, which is the most precise measurement ever obtained.

References

1. Andronic, A.; Braun-Munzinger, P.; Stachel, J.; Stocker, H. Production of light nuclei, hypernuclei and their antiparticles in relativistic nuclear collisions. *Phys. Lett. B* **2011**, *697*, 203, doi:10.1016/j.physletb.2011.01.053.
2. Kapusta, J.I. Mechanisms for deuteron production in relativistic nuclear collisions. *Phys. Rev. C* **1980**, *21*, 1301, doi:10.1103/PhysRevC.21.1301.
3. Rayet, M.; Dalitz, R.H. The lifetime of 3H*v*. *Nuovo Cim. A* **1966**, *46*, 786.
4. Congleton, J.G. A Simple model of the hypertriton. *J. Phys. G* **1992**, *18*, 339, doi:10.1088/0954-3899/18/2/015.
5. Kamada, H.; Golak, J.; Miyagawa, K.; Witala, H.; Gloeckle, W. Pi mesonic decay of the hypertriton. *Phys. Rev. C* **1998**, *57*, 1595, doi:10.1103/PhysRevC.57.1595.
6. Abelev, B.B. et al. [ALICE Collaboration]. Performance of the ALICE Experiment at the CERN LHC. *Int. J. Mod. Phys. A* **2014**, *29*, 1430044, doi:10.1142/S0217751X14300440.
7. Adam, J. et al. [ALICE Collaboration]. Production of light nuclei and anti-nuclei in pp and Pb-Pb collisions at energies available at the CERN Large Hadron Collider. *Phys. Rev. C* **2016**, *93*, 024917, doi:10.1103/PhysRevC.93.024917.
8. Tsallis, C. Possible Generalization of Boltzmann-Gibbs Statistics. *J. Statist. Phys.* **1988**, *52*, 479, doi:10.1007/BF01016429.
9. Schnedermann, E.; Sollfrank, J.; Heinz, U.W. Thermal phenomenology of hadrons from 200-A/GeV S+S collisions. *Phys. Rev. C* **1993**, *48*, 2462, doi:10.1103/PhysRevC.48.2462.